A novel set-up for the ex vivo analysis of mechanical properties of mouse aortic segments stretched at physiological pressure and frequency

A novel set-up for the *ex vivo* analysis of mechanical properties of mouse aortic segments stretched at physiological pressure and frequency.

Arthur J.A. Leloup[1], Cor E. Van Hove[2], Ammar Kurdi[1], Sofie De Moudt[1], Wim Martinet[1], Guido RY De Meyer[1], Dorien M. Schrijvers[1], Gilles W. De Keulenaer[1], Paul Fransen[1]

1: University of Antwerp, Department of Pharmaceutical Sciences, Laboratory of Physiopharmacology, Campus Drie Eiken, Universiteitsplein 1, B-2610 Antwerp, Belgium

2: University of Antwerp, Faculty of Medicine and Health Sciences, Laboratory of Pharmacology, Campus Drie Eiken, Universiteitsplein 1, B-2610 Antwerp, Belgium

Corresponding author: Arthur Leloup, University of Antwerp, Department of Pharmaceutical Sciences, Campus Drie Eiken, Laboratory of Physiopharmacology, Universiteitsplein 1, B-2610 Antwerp, Belgium

Telephone: +32 3 265 25 71, Fax: +32 3 265 25 67, E-mail: Arthur.Leloup@uantwerpen.be

RUNNING TITLE: Mechanical properties of periodically stretched mouse aortic segments

KEY WORDS: aortic stiffness, cyclic stretch, basal NO, VSMC tone

KEY POINTS

- Cyclic stretch is known to alter intracellular pathways involved in vessel tone regulation.
- We developed a novel set-up that allows straightforward characterization of the biomechanical properties of the mouse aorta while stretched at a physiological rate (600 bpm).
- Active vessel tone was shown to have surprisingly large effects on isobaric stiffness
- The effect of structural vessel wall alterations was confirmed using a genetic mouse model.
- This set-up will contribute to a better understanding of how active vessel wall components and mechanical stimuli such as stretch frequency and amplitude regulate aortic mechanics.

ABSTRACT

Cyclic stretch is a major contributor of vascular function. However, isolated mouse aortas are frequently studied at low stretch frequency or even isometric conditions. Pacing experiments in rodents and humans show that arterial compliance is stretch frequency-dependent. The Rodent Oscillatory Tension Set-up to study Arterial Compliance is an in-house developed organ bath set-up that clamps aortic segments to imposed preloads at physiological rates up to 600bpm. The technique enables us to derive pressure-diameter loops and assess biomechanical properties of the segment. To validate the applicability of this set-up we aimed to confirm the effects of distension pressure and vascular smooth muscle tone on arterial stiffness. At physiological stretch frequency (10 Hz), Peterson modulus (293 (10) mmHg) for wild-type mouse aorta increased 22% upon a rise in pressure from 80-120 mmHg to 100-140 mmHg, while, at normal pressure, Ep increased 80% upon maximal contraction of the vascular smooth muscle cells. We further validated the method using a mouse model with a mutation in the Fibrillin-1 gene and an endothelial nitric oxide synthase knock-out model. Both models are known to have increased arterial stiffness, and this was confirmed using the set-up.

To our knowledge, this is the first set-up that facilitates the study of biomechanical properties of mouse aortic segments at physiological stretch frequency and pressure. We believe that this set-up can contribute to a better understanding of how cyclic stretch frequency, amplitude and active vessel wall components influence arterial stiffening.

ABBREVIATIONS

CV, cardiovascular; eNOS, endothelial nitric oxide synthase; L-NAME, NΩ-nitro-l-arginine methyl ester; NO, nitric oxide; PE, phenylephrine; ROTSAC, Rodent Oscillatory Tension Set-up to study Arterial Compliance; VSMC, vascular smooth muscle cell;

INTRODUCTION

Progressive large artery stiffening is the predominant cause of increased pulse pressure, a marker of cardiovascular (CV) risk in the general population (Benetos *et al.*, 1997) and a predictor of CV events (Mitchell *et al.*, 1997). Furthermore, it reduces myocardial perfusion efficiency, increases left ventricular afterload and elicits mechanical stress on capillaries, potentially damaging the capillary wall of strongly perfused organs such as the heart, brain and kidneys (Safar *et al.*, 2012). It is generally assumed that arterial stiffness is an adaptation mechanism of the aortic wall to increased distending pressures. However, the REASON study, published in 2009, states that, in hypertensive patients, high arterial stiffness predicts a poor response to antihypertensive treatment (Protogerou *et al.*, 2009). In addition, several epidemiological studies report that arterial stiffness precedes hypertension in the elderly (Najjar *et al.*, 2008; Kaess *et al.*, 2012). This temporal relationship was recently confirmed in a mouse model of diet-induced obesity; i.e. arterial stiffness preceded hypertension and target organ damage in this model (Weisbrod *et al.*, 2013). These observations suggest a role for arterial stiffness as a therapeutic target to treat CV disease.

In recent years, there is emerging evidence that not only passive components determine arterial compliance. Indeed, vascular smooth muscle cell (VSMC) stiffness and active vessel wall components (i.e. nitric oxide (NO) bioavailability and VSMC tonus) also affect arterial compliance (Fitch *et al.*, 2001; Kinlay *et al.*, 2001; Bellien *et al.*, 2010; Sehgel *et al.*, 2013). Although the interest in these pathways as potential therapeutic targets has grown, their definite role in arterial stiffening during disease processes is still incompletely understood, increasing the need for further research on active vessel wall components in arterial stiffening. Several *in vivo* techniques to measure arterial stiffness are available (Hartley *et al.*, 1997; Herold *et al.*, 2009; Leloup *et al.*, 2014; Di Lascio *et al.*, 2014) but in order to analyse the underlying molecular pathways, *ex vivo* analysis with manipulation of the experimental environment is required. *Ex vivo* perfusion of artery segments is frequently used to assess biomechanical parameters (Huang *et al.*, 2008; Le *et al.*, 2011), but the lack of cyclic stretch may alter endothelial NO synthase (eNOS) activity, especially since aortic endothelial cells are sensitive to cyclic stretch–amplitude (Peng *et al.*, 2003) and that heart rate is a blood pressure-independent determinant of aortic stiffness (Millasseau *et al.*, 2005; Tan *et al.*, 2012). In addition, arteries are known to show

viscoelastic behaviour as indicated by the hysteresis phenomenon in the pressure-diameter plot (Boutouyrie *et al.*, 1997) and this depends on the frequency of stretching. Indeed, when stretch frequency is low, the pressure-diameter relationship is linear and hysteresis is absent (Santelices *et al.*, 2007). The viscosity of the artery is thought to be a major contributor to the pulse-smoothening capacity of the aorta, indicating that the study of VSMC tone and aortic mechanics under isometric conditions in the commonly used wire or perfusion myograph set-ups may be biased. Pulsatile perfusion can be applied but, given the high heart rate and small size of the mouse, this is generally applied to larger animal models such as the rat (Boutouyrie *et al.*, 1997) and sheep (Bia *et al.*, 2005). A set-up that exposes mouse aortic segments to pulsatile perfusion is reported but only with subphysiological stretch rate (20bpm) (Santelices *et al.*, 2007).

Therefore, we aimed to develop a novel *ex vivo* approach to study elastic behaviour of aortic segments while stretched at physiological frequencies and amplitudes. The Rodent Oscillatory Tension Set-up to study Arterial Compliance (ROTSAC) is an organ bath set-up with the aortic segment connected to a force-length transducer which allows clamping the segments at different preloads. A stretch protocol was applied with physiological frequency (10 Hz) and amplitude (40 mmHg). We aimed to i) estimate the reproducibility of the set-up ii) confirm the *ex vivo* effect of increased distension pressure and VMSC tone on stiffness parameters, iii) assess aortic stiffness of isolated aortic segments from two genetic mouse models known to have increased aortic stiffness and iv) test whether physical integrity of the isolated aortic segment is morphologically and mechanically maintained when high frequency oscillation is applied.

MATERIALS AND METHODS

Ethical approval

The studies were approved by the Ethical Committee of the University of Antwerp, and all experiments were performed conform to the Guide for the Care and Use of Laboratory Animals published by the US National Institutes of Health (NIH Publication No. 85–23, revised 1996).

Animals

All animals (C57Bl/6J background) were bred and housed in the animal facility of the University of Antwerp in standard cages with 12h-12h light-dark cycles with free access to regular chow and tap water. The length and diameter calibration method was validated using 8 aortic segments from 4 male WT mice 28.0 (1.2) g. For the other experiments, 5 male WT mice 22.5 (2.0) g, 5 male $eNOS^{-/-}$ mice 30.6 (3.4) g and 4 male $ApoE^{-/-}Fbn1^{C1039G+/-}$ (Fbn-1-mut, 32.7 (0.8) g) were used. Animals were euthanized by perforating the diaphragm while under anaesthesia (sodium pentobarbital (Sanofi, Belgium), 75 mg kg^{-1}, i.p.). The thoracic aorta was carefully removed and stripped of adherent tissue. Starting at the diaphragm, the aorta was cut in 6 segments of 2 mm width. The 3th and 4th segment were immersed in Krebs Ringer solution (37°C, 95% O_2/5% CO_2, pH 7.4) containing (in mM): NaCl 118, KCl 4.7, $CaCl_2$ 2.5, KH_2PO_4 1.2, $MgSO_4$ 1.2, $NaHCO_3$ 25, CaEDTA 0.025 and glucose 11.1. To avoid any vasomotor interference due to prostanoids, 10 µM indomethacin (Federa, Belgium) was present in all experiments.

ROTSAC

Aortic segments were mounted between two parallel wire hooks in 8 mL organ baths. Force and displacement of the upper hook were controlled and measured with a force-length transducer described earlier (Brutsaert *et al.*, 1971; Brutsaert & Claes, 1974). In short, the upper hook was connected to the aluminium lever of the force-length transducer. This lever was connected to a coil suspended in a strong field of a permanent magnet. The system was controlled by a current source. When current was passed through this coil, a force was developed. The displacement of the lever was measured by means of a photo-electric system. The transducer was connected to a data acquisition system (Powerlab 8/30 and LabChart 7, ADInstruments) (Figure 1). Force and displacement were acquired at 1 kHz. To calculate the transmural pressure that would exist in the equilibrated vessel segment with the given wall stress (derived from the distension force) and dimensions, the Laplace relationship was used:

$$P = \frac{F}{l.D}$$

with F the force, l the length and D the diameter of the vessel segment. Force was measured directly by the transducer. The diameter of the vessel segment at a given preload was derived from the displacement of the upper hook, being directly proportional to the inner circumference:

$$D = \frac{2g}{\pi}$$

with g the outer distance between the hooks (to approximate the inner circumference of the vessel segment). Before each experiment, diameter and length were determined at three different preloads (20, 40 and 60 mN) using a binocular and calibrated image software. To correct for the slight decrease in vessel length with increased diameter, the average length per cycle (100 ms) was derived from the diameter-length relationship using linear regression.

The preload was adjusted until the desired calculated diastolic and systolic pressure. The acquired pressure-diameter loops were used for further analysis. Compliance (C) was calculated as follows:

$$C = \frac{\Delta D}{\Delta P}$$

with ΔD, the difference between systolic and diastolic diameter and ΔP, the pressure difference (+/- 40 mmHg in the present study). The Peterson modulus of elasticity (E_p) is a frequently used, vessel size-independent measure of arterial stiffness (Gosling & Budge, 2003) and was calculated as follows:

$$Ep = D_0 . \frac{\Delta P}{\Delta D}$$

with D_0, the diastolic diameter. During all experiments, the segments were periodically stretched directly after mounting them in the organ bath with a frequency of 10 Hz to mimic the physiological heart rate in mice (600 bpm). VSMCs were stimulated using the α_1-adrenergic agonist phenylephrine (PE) (Sigma-Aldrich, Belgium) and NΩ-nitro-l-arginine methyl ester (L-NAME) (Sigma-Aldrich, Belgium) was used to inhibit eNOS.

Histology

Segments, which were mounted in the ROTSAC for 4 hours with or without repetitive stretching (10 Hz) at preloads corresponding to normal pressures, were formalin-fixed for 24 hours, dehydrated overnight in 60% isopropanol and embedded in paraffin. Histological analysis was performed on serial cross sections (5µm) stained with orcein to visualize elastin. The images

were acquired with the Universal Grab 6.1. (IDL) software (Exelis, Boulder, CO) using an Olympus BX40 microscope (Tokyo, Japan).

Statistical analysis

All results are expressed as mean (SD) or median (interquartile range) with n representing the number of mice and analysed using GraphPad Prism 6.0. Data of the VSMC tone and pressure effect were compared by two-way ANOVA with Bonferroni multiple comparison post-hoc test. The genetic mouse models with arterial stiffness were compared against WT mice using a Mann-Whitney U test. The effect of the 4 hours stretch protocol on Ep was evaluated using a paired t-test. A 5% level of significance was selected.

RESULTS

1. Vessel dimensions are accurately derived from the force-length transducer

Effective diameter and length were determined at different preloads using a binocular and compared with the calculated diameter derived from the displacement of the upper hook. Bland-Altman analysis revealed a bias of -10.73 µm on the estimation of the diameter (0.9 % of the mean diameter. The 95% limits of agreement were -44.6 µm (3.9% of the mean diameter) and +23.2 µm (2.1% of the mean diameter) (Figure 2A, B)). When length was determined using the diameter-length relationship, the bias was -4.3 µm (0.3 % of the mean length) and 95 % limits of agreement were -34.4 µm (2.0 % of the mean) and +25.8 µm (0.9 % of the mean length) (Figure 2C, D). Overall, both estimations of length and diameter were considered sufficiently accurate and this method of estimating vessel dimensions was used to determine the calculated transmural pressure. Figure 3 shows the diameter-time plot (Figure 3A) of a compliant and a stiff vessel segment. The hysteresis phenomenon typically seen when stretching vessel segments at sufficiently high frequency is apparent from the resulting pressure-diameter plot (Figure 3B).

2. The ROTSAC allows isobaric assessment of mechanical properties of aortic segments with different VSMC tone or at different distension pressures.

Because distension pressure and VSMC tone are known modulators of aortic stiffness, we tested whether this set-up was able to pick up changes in biomechanical properties induced by pharmacological stimulation of VSMCs, both at normal pressure (80-120 mmHg) and higher pressure (100-140 mmHg). Upon pharmacological stimulation of α1-adrenergic receptors with 1 µM phenylephrine (PE), diastolic diameter (D_0) significantly decreased and both diameter-dependent and diameter-independent parameters changed significantly (Figure 4). This effect was even more pronounced when the basal production of the relaxing factor NO was inhibited using 300 µM L-NAME. As expected, increased distending pressure significantly changed the mechanical properties of the aortic segment for all conditions (Figure 4).

3. The ROTSAC confirms altered mechanical properties in aortic segments of two genetic mouse models.

To test the capacity of the set-up to pick up differences in arterial stiffness between mouse models with known altered aortic geometry and mechanics, a mouse model with a mutation in the Fbn1 gene was used (Van der Donckt *et al.*, 2015). The aortic diameter was increased as compared to WT mice (Figure 5A). Relative distension (Figure 5B) and compliance (Figure 5C) were significantly lower and Ep was significantly increased at physiological pressure (Figure 5D).

Next, aortic segments from $eNOS^{-/-}$ mice – as a second model known to have increased arterial stiffness – were analyzed. Although aortic diameter was similar to aortae from WT mice (Figure 6A), relative distension (Figure 6B), compliance (Figure 6C) and Ep (Figure 6D) were significantly different in $eNOS^{-/-}$ mice.

4. Functional and physical integrity of the vessel segment is maintained over time

The effect of repetitive stretching on elastin fibre integrity was evaluated on sections of segments after being mounted for 4 hours in the ROTSAC set-up with or without stretching (10 Hz, physiological pressure). No differences in general morphology were observed on H&E stained sections (data not shown). Orcein-stained aortic sections revealed no difference in elastin fibre integrity after stretching (Figure 7A, B) and Ep did not change significantly after a 4 hour stretch protocol on aortic segments from both WT and $eNOS^{-/-}$ mice. These data indicate that repetitive stretching does not damage the elastin fibres in the organ bath.

DISCUSSION

In the present paper, we describe the validation of a novel organ bath set-up that allows the assessment of isobaric stiffness parameters while cyclic stretch is applied at a physiological frequency. This is potentially important as several studies suggest that aortic mechanics are regulated by cyclic stretch in an amplitude and frequency-dependent matter (Lantelme, 2002; Peng *et al.*, 2003; Tan *et al.*, 2012).

All vertebrates and invertebrates with a closed circulatory system have arteries that show non-linear elasticity. In the present study, this intrinsic property of the aorta was used to validate the sensitivity of the set-up to detect changes due to increased distension pressure. Measurements were done at normal (80-120 mmHg) and increased (100-140 mmHg) pressure, while keeping the stretch frequency and amplitude the same. In basal conditions, Ep increased by 20 % with increased pressure and the effect of pressure remained significant for all conditions.

Traditionally, passive vessel wall components such as elastin and collagen fibres are considered the most important determinants of arterial stiffness. However, active components that modulate VSMC tone are also known to play an important role (Wilkinson & McEniery, 2004). Therefore, we pharmacologically modulated VSMC tone to test the sensitivity of our set-up to pick up these changes. Contraction of VSMCs using PE significantly increased isobaric stiffness. When the production of NO was blocked in PE-stimulated segments, isobaric stiffness increased by 80% as compared to baseline. This large effect of eNOS inhibition can be expected since we reported earlier that, in contrast to muscular arteries, the elastic arteries such as the aorta, produce large amounts of NO in basal conditions (Leloup *et al.*, 2015). This was also suggested by *in vivo* experiments in rodent models and humans that demonstrated the direct link between (basal) NO production and arterial stiffness (Kinlay *et al.*, 2001; Wilkinson *et al.*, 2002; Schmitt *et al.*, 2005; Isabelle *et al.*, 2012).

To further confirm the ability of our set-up to pick up differences in aortic stiffness, we used two genetic mouse models. We were able to demonstrate an increased aortic diameter and increased stiffness in segments of the $ApoE^{-/-}Fbn1^{C1039G/+}$ aorta. Indeed, isometric wire myograph analysis

demonstrated a steeper stress-strain relationship in 20 weeks old $ApoE^{-/-}Fbn1^{C1039G/+}$ mice (Van Herck *et al.*, 2009) and histological analysis revealed a lower elastin content, increased elastin fragmentation and vessel diameter (Van der Donckt *et al.*, 2015).

In aortae from $eNOS^{-/-}$ mice, stiffness parameters were significantly increased while aortic diameter was similar to aortic segments from WT mice. We and others previously showed increased pulse wave velocity – an important *in vivo* parameter of arterial stiffness – in $eNOS^{-/-}$ mice (Soucy *et al.*, 2006; Leloup *et al.*, 2014) and the stress-strain relationship of aortic segments of $eNOS^{-/-}$ mice was steeper as compared to WT mice (Jung *et al.*, 2013).

These data illustrate the applicability and validity of the ROTSAC set-up to measure biomechanical properties of isolated mouse aortic segments. In contrast to *in vivo* analyses of pressure diameter relationships (Giannattasio *et al.*, 2008; Vayssettes-Courchay *et al.*, 2011) that provide local biomechanical and visco-elastic information in a physiological environment, the *ex vivo* ROTSAC set-up, in which segments of the aorta are isolated, allows to independently alter the distension pressure, pulse pressure, stretch frequency and the composition of the extracellular fluid. Thereby, the effects of VSMC tone, pulse pressure, stretch frequency and distension pressure can be separately investigated to study the active regulation of aortic compliance. Nevertheless, some disadvantages are inevitably linked to the lack of perfusion. Firstly, similar organ bath set-ups based on perfusion allow direct measurement of luminal pressure, while this set-up relies on indirect calculations using the Laplace relationship, assuming a thin, isotropic and homologous wall. The mouse aorta does not meet these assumptions so one should be cautious when interpreting absolute values of calculated pressure. However, the Laplace relationship has been used extensively before in ex-vivo biomechanical analysis of the mouse aorta (Syyong *et al.*, 2009; Van Herck *et al.*, 2009; Butlin *et al.*, 2015) and here we confirm that it provides a sufficiently sensitive and practical method to estimate transluminal pressure to evaluate the effects of distension pressure and VSMC tone. Secondly, perfusion-based set-ups expose the endothelial cells to shear stress, a well-known stimulator of endothelial NO production. As mentioned before, we reported that elastic arteries of the mouse produce large amounts of basal NO *in vitro*. Only very recently we observed that repetitive stretching of the isolated mouse aorta increased basal NO production even more in an amplitude-dependent manner (unpublished data).

Although it is assumed that shear stress is homogeneously distributed in the arterial tree, a review of the literature of shear stress measurements in healthy volunteers revealed that shear stress is lower in the aorta versus other parts of the arterial tree (Pantos *et al.*, 2007). These observations indicate that the contribution of shear stress is more important in the muscular arteries to regulate vessel diameter and, hence, flow, while the elastic arteries – where cyclic deformation is larger – rely more on stretch-dependent and basal NO production to keep VSMC tone low and the pulse smoothening capacity of the aorta high (Leloup *et al.*, 2015). To determine the relative contribution of basal NO production, cyclic stretch and shear stress-dependent NO production in the different vessel types, further research is required. Thirdly, upon isolating the aorta, neurogenic and hormonal stimuli are lost and these have been shown to play a role in the regulation of large artery mechanics (Pagani *et al.*, 1975; Barra *et al.*, 1993). A study that compared the effects of vasoactive substances on the aorta found large differences *in vivo* versus *ex vivo* (Butlin *et al.*, 2015) and visco-elastic properties of the aorta change significantly after isolation of the aorta from the animal (Boutouyrie *et al.*, 1997). Therefore, one should be cautious when translating observations from *ex vivo* set-ups such as the ROTSAC to the physiological *in vivo* setting as the combined action of mechanical, neurogenic and hormonal stimuli may differ.

Overall, we were able to show that this set-up allows fast and straightforward assessment of the intrinsic mechanical and geometrical properties of aortic segments *ex vivo*. We confirmed the dependency of aortic stiffness on distension pressure and demonstrated large effects of increased VSMC tone on arterial stiffness in aortic segments of WT mice. Two mouse models with known increased arterial stiffness were used to further assess the sensitivity of the set-up and known differences in vessel mechanics were confirmed. In contrast to (pulsatile) perfusion-based set-ups, only a limited amount of tissue is required (1-2 mm aortic segments), allowing parallel testing of multiple conditions, thereby drastically reducing the number of animals required. The aforementioned properties of this set-up are novel and complementary with perfusion-based *ex vivo* set-ups or *in vivo* pressure-diameter loop analysis. It will facilitate future research how active vessel wall components (endothelial and VSMC crosstalk) and mechanical stimuli such as distension pressure, pulse pressure and frequency affect arterial biomechanics. More knowledge about the role of these factors in arterial aging, exercise and hypertension is crucial for the

development of specific de-stiffening strategies that are believed to play a crucial role in future cardiovascular health management.

COMPETING INTERESTS

The authors declare that they have no competing interests.

AUTHOR CONTRIBUTIONS

AL, CVH and PF conceived and designed the experiments. Acquisition, analysis, and interpretation of data was carried out by AL, CVH, AK, SDM and PF in the laboratories of WM, GDM, DS, GDK and PF. The manuscript was drafted and critically revised by AL, CVH, AK, SDM, WM, GDM, DS, GDK and PF. All authors have approved the final version of the manuscript and agree to be accountable for all aspects of the work. All persons designated as authors qualify for authorship, and all those who qualify for authorship are listed.

FUNDING

AL is supported by the Fund for Scientific Research (FWO) Flanders, grant number 11W3716N.

ACKNOWLEDGEMENTS

The electronic design of the ROTSAC set-ups was done by Victor Claes and Bart Geraets (ACTUR, Edegem, Belgium).

REFERENCES

Barra JG, Armentano RL, Levenson J, Fischer EI, Pichel RH & Simon A (1993). Assessment of smooth muscle contribution to descending thoracic aortic elastic mechanics in conscious dogs. *Circ Res* **73,** 1040–1050.

Bellien J, Favre J, Iacob M, Gao J, Thuillez C, Richard V & Joannidès R (2010). Arterial stiffness is regulated by nitric oxide and endothelium-derived hyperpolarizing factor during changes in blood flow in humans. *Hypertension* **55,** 674–680.

Benetos A, Safar M, Rudnichi A, Smulyan H, Richard JL, Ducimetieère P & Guize L (1997). Pulse pressure: a predictor of long-term cardiovascular mortality in a French male population. *Hypertension* **30,** 1410–1415.

Bia D, Aguirre I, Zócalo Y, Devera L, Cabrera Fischer E & Armentano R (2005). Regional Differences in Viscosity, Elasticity, and Wall Buffering Function in Systemic Arteries: Pulse Wave Analysis of the Arterial Pressure-Diameter Relationship. *Rev Española Cardiol* **58,** 167–174.

Boutouyrie P, Bézie Y, Lacolley P, Challande P, Chamiot-Clerc P, Benetos A, de la Faverie JF, Safar M & Laurent S (1997). In vivo/in vitro comparison of rat abdominal aorta wall viscosity. Influence of endothelial function. *Arterioscler Thromb Vasc Biol* **17,** 1346–1355.

Brutsaert DL & Claes VA (1974). Onset of mechanical activation of mammalian heart muscle in calcium- and strontium-containing solutions. *Circ Res* **35,** 345–357.

Brutsaert DL, Claes VA & Sonnenblick EH (1971). Effects of abrupt load alterations on force-velocity-length and time relations during isotonic contractions of heart muscle: load clamping. *J Physiol* **216,** 319–330.

Butlin M, Lindesay G, Viegas KD & Avolio AP (2015). Pressure dependency of aortic pulse wave velocity in vivo is not affected by vasoactive substances that alter aortic wall tension ex vivo. *Am J Physiol Heart Circ Physiol* **308,** H1221–H1228.

Van der Donckt C et al. (2015). Elastin fragmentation in atherosclerotic mice leads to intraplaque neovascularization, plaque rupture, myocardial infarction, stroke, and sudden death. *Eur Heart J* **36,** 1049–1058.

Fitch RM, Vergona R, Sullivan ME & Wang YX (2001). Nitric oxide synthase inhibition increases aortic stiffness measured by pulse wave velocity in rats. *Cardiovasc Res* **51,** 351–358.

Giannattasio C, Salvi P, Valbusa F, Kearney-Schwartz A, Capra A, Amigoni M, Failla M, Boffi L, Madotto F, Benetos A & Mancia G (2008). Simultaneous measurement of beat-to-beat carotid diameter and pressure changes to assess arterial mechanical properties. *Hypertension* **52,** 896–902.

Gosling RG & Budge MM (2003). Terminology for describing the elastic behavior of arteries.

Hypertension **41,** 1180–1182.

Hartley CJ, Taffet GE, Michael LH, Pham TT & Entman ML (1997). Noninvasive determination of pulse-wave velocity in mice. *Am J Physiol* **273,** H494–H500.

Van Herck JL, De Meyer GRY, Martinet W, Van Hove CE, Foubert K, Theunis MH, Apers S, Bult H, Vrints CJ & Herman AG (2009). Impaired fibrillin-1 function promotes features of plaque instability in apolipoprotein E-deficient mice. *Circulation* **120,** 2478–2487.

Herold V, Parczyk M, Mörchel P, Ziener CH, Klug G, Bauer WR, Rommel E & Jakob PM (2009). In vivo measurement of local aortic pulse-wave velocity in mice with MR microscopy at 17.6 Tesla. *Magn Reson Med* **61,** 1293–1299.

Huang Y, Guo X & Kassab GS (2008). Relation of nitrite to structural and mechanical adaptation of arteries during postnatal development. *Ann Biomed Eng* **36,** 2019–2027.

Isabelle M, Simonet S, Ragonnet C, Sansilvestri-Morel P, Clavreul N, Vayssettes-Courchay C & Verbeuren TJ (2012). Chronic reduction of nitric oxide level in adult spontaneously hypertensive rats induces aortic stiffness similar to old spontaneously hypertensive rats. *J Vasc Res* **49,** 309–318.

Jung SM, Jandu S, Steppan J, Belkin A, An SS, Pak A, Choi EY, Nyhan D, Butlin M, Viegas K, Avolio A, Berkowitz DE & Santhanam L (2013). Increased tissue transglutaminase activity contributes to central vascular stiffness in eNOS knockout mice. *Am J Physiol Heart Circ Physiol* **305,** H803–H810.

Kaess BM, Rong J, Larson MG, Hamburg NM, Vita JA, Levy D, Benjamin EJ, Vasan RS & Mitchell GF (2012). Aortic stiffness, blood pressure progression, and incident hypertension. *JAMA* **308,** 875–881.

Kinlay S, Creager MA, Fukumoto M, Hikita H, Fang JC, Selwyn AP & Ganz P (2001). Endothelium-Derived Nitric Oxide Regulates Arterial Elasticity in Human Arteries In Vivo. *Hypertension* **38,** 1049–1053.

Lantelme P (2002). Heart Rate: An Important Confounder of Pulse Wave Velocity Assessment. *Hypertension* **39,** 1083–1087.

Di Lascio N, Stea F, Kusmic C, Sicari R & Faita F (2014). Non-invasive assessment of pulse wave velocity in mice by means of ultrasound images. *Atherosclerosis* **237,** 31–37.

Le VP, Knutsen RH, Mecham RP & Wagenseil JE (2011). Decreased aortic diameter and compliance precedes blood pressure increases in postnatal development of elastin-insufficient mice. *Am J Physiol Heart Circ Physiol* **301,** H221–H229.

Leloup AJA, Fransen P, Van Hove CE, Demolder M, De Keulenaer GW & Schrijvers DM (2014). Applanation Tonometry in Mice: A Novel Noninvasive Technique to Assess Pulse Wave Velocity and Arterial Stiffness. *Hypertension* **64,** 195–200.

Leloup AJA, Van Hove CE, Heykers A, Schrijvers DM, De Meyer GRY & Fransen P (2015). Elastic and Muscular Arteries Differ in Structure, Basal NO Production and Voltage-Gated

Ca2+-Channels. *Front Physiol* **6,** 375.

Millasseau SC, Stewart AD, Patel SJ, Redwood SR & Chowienczyk PJ (2005). Evaluation of carotid-femoral pulse wave velocity: influence of timing algorithm and heart rate. *Hypertension* **45,** 222–226.

Mitchell GF, Moyé LA, Braunwald E, Rouleau JL, Bernstein V, Geltman EM, Flaker GC & Pfeffer MA (1997). Sphygmomanometrically determined pulse pressure is a powerful independent predictor of recurrent events after myocardial infarction in patients with impaired left ventricular function. SAVE investigators. Survival and Ventricular Enlargement. *Circulation* **96,** 4254–4260.

Najjar SS, Scuteri A, Shetty V, Wright JG, Muller DC, Fleg JL, Spurgeon HP, Ferrucci L & Lakatta EG (2008). Pulse wave velocity is an independent predictor of the longitudinal increase in systolic blood pressure and of incident hypertension in the Baltimore Longitudinal Study of Aging. *J Am Coll Cardiol* **51,** 1377–1383.

Pagani M, Schwartz PJ, Bishop VS & Malliani A (1975). Reflex sympathetic changes in aortic diastolic pressure-diameter relationship. *Am J Physiol* **229,** 286–290.

Pantos I, Patatoukas G, Efstathopoulos EP & Katritsis D (2007). In vivo wall shear stress measurements using phase-contrast MRI. *Expert Rev Cardiovasc Ther* **5,** 927–938.

Peng X, Haldar S, Deshpande S, Irani K & Kass DA (2003). Wall stiffness suppresses Akt/eNOS and cytoprotection in pulse-perfused endothelium. *Hypertension* **41,** 378–381.

Protogerou A, Blacher J, Stergiou GS, Achimastos A & Safar ME (2009). Blood Pressure Response Under Chronic Antihypertensive Drug Therapy. *J Am Coll Cardiol* **53,** 445–451.

Safar ME, Nilsson PM, Blacher J & Mimran A (2012). Pulse pressure, arterial stiffness, and end-organ damage. *Curr Hypertens Rep* **14,** 339–344.

Santelices LC, Calano SJ, Erhart JC, Prantil RL, Haney JL, Vorp DA & Ahearn JM (2007). Experimental system for ex vivo measurement of murine aortic stiffness. *Physiol Meas* **28,** N39–N49.

Schmitt M, Avolio A, Qasem A, McEniery CM, Butlin M, Wilkinson IB & Cockcroft JR (2005). Basal NO Locally Modulates Human Iliac Artery Function In Vivo. *Hypertension* **46,** 227–231.

Sehgel NL, Zhu Y, Sun Z, Trzeciakowski JP, Hong Z, Hunter WC, Vatner DE, Meininger GA & Vatner SF (2013). Increased vascular smooth muscle cell stiffness: a novel mechanism for aortic stiffness in hypertension. *Am J Physiol Heart Circ Physiol* **305,** H1281–H1287.

Soucy KG, Ryoo S, Benjo A, Lim HK, Gupta G, Sohi JS, Elser J, Aon M a, Nyhan D, Shoukas AA & Berkowitz DE (2006). Impaired shear stress-induced nitric oxide production through decreased NOS phosphorylation contributes to age-related vascular stiffness. *J Appl Physiol* **101,** 1751–1759.

Syyong HT, Chung AWY, Yang HHC & van Breemen C (2009). Dysfunction of endothelial and

smooth muscle cells in small arteries of a mouse model of Marfan syndrome. *Br J Pharmacol* **158,** 1597–1608.

Tan I, Butlin M, Liu YY, Ng K & Avolio AP (2012). Heart rate dependence of aortic pulse wave velocity at different arterial pressures in rats. *Hypertension* **60,** 528–533.

Vayssettes-Courchay C, Ragonnet C, Isabelle M & Verbeuren TJ (2011). Aortic stiffness in vivo in hypertensive rat via echo-tracking: analysis of the pulsatile distension waveform. *Am J Physiol Heart Circ Physiol* **301,** H382–H390.

Weisbrod RM, Shiang T, Al Sayah L, Fry JL, Bajpai S, Reinhart-King CA, Lob HE, Santhanam L, Mitchell G, Cohen RA & Seta F (2013). Arterial Stiffening Precedes Systolic Hypertension in Diet-Induced Obesity. *Hypertension* **62,** 1105–1110.

Wilkinson IB & McEniery CM (2004). Arterial stiffness, endothelial function and novel pharmacological approaches. *Clin Exp Pharmacol Physiol* **31,** 795–799.

Wilkinson IB, Qasem A, McEniery CM, Webb DJ, Avolio AP & Cockcroft JR (2002). Nitric oxide regulates local arterial distensibility in vivo. *Circulation* **105,** 213–217.

FIGURE LEGENDS

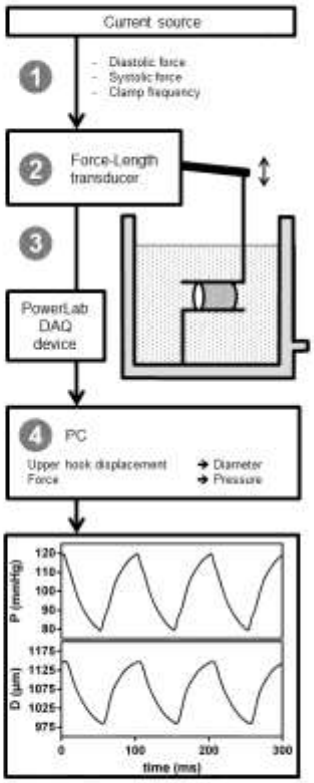

Figure 1. Schematic diagram of the ROTSAC. The aortic segment was mounted between two metal hooks in an organ bath. (1) A current source was used to control the distension force and clamp frequency (10 Hz) of the force-length transducer. Force and displacement were measured by the transducer (2) and acquired at 1 kHz by a PowerLab DAQ device (3). Diameter, length and force were used to calculate the pressure that would exist in an equilibrated vessel segment with the given dimensions and wall stress (4).

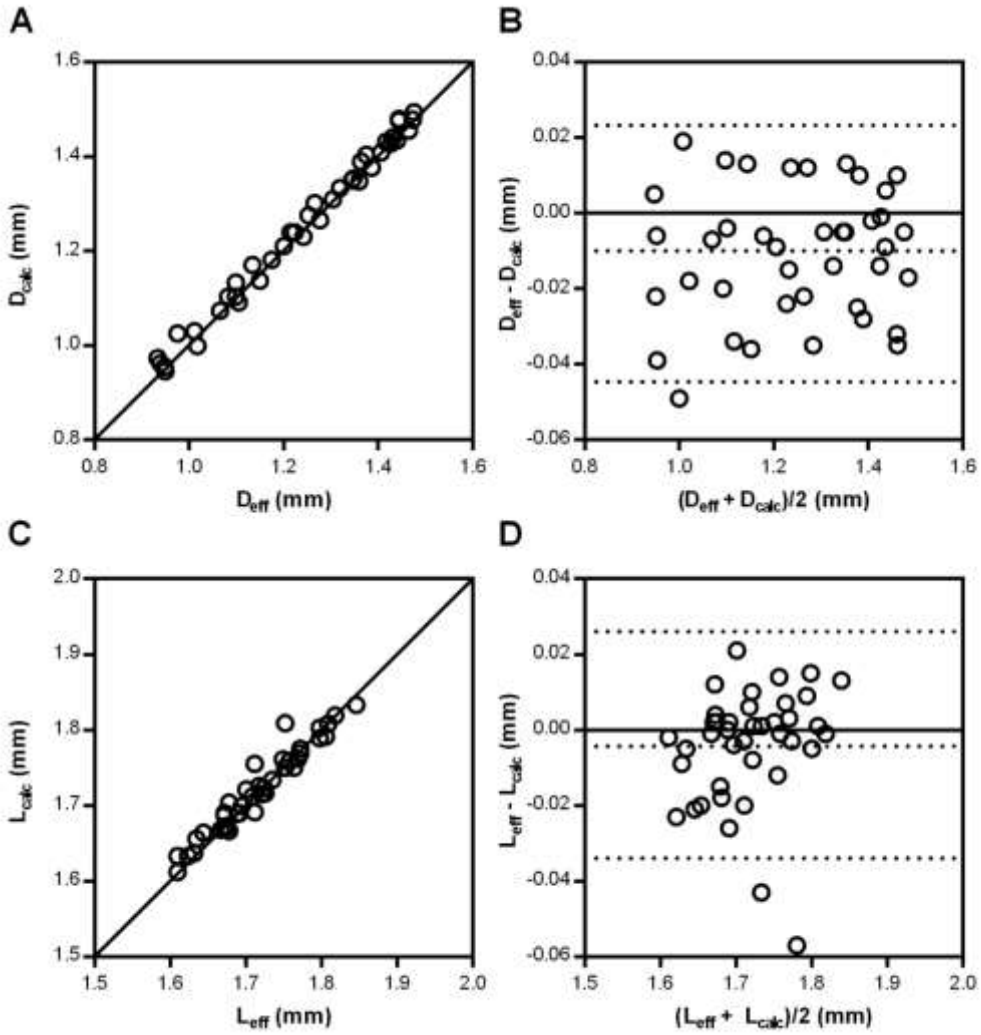

Figure 2. Bland-Altman analysis of geometrical parameters. Comparison between effective diameter (D_{eff}) (A, B) and length (L_{eff}) (C, D) and the calculated parameters (D_{calc}, L_{calc}) derived from the displacement of the needle and the diameter-length relationship, respectively. The dashed lines represent the bias and 95% limits of agreement.

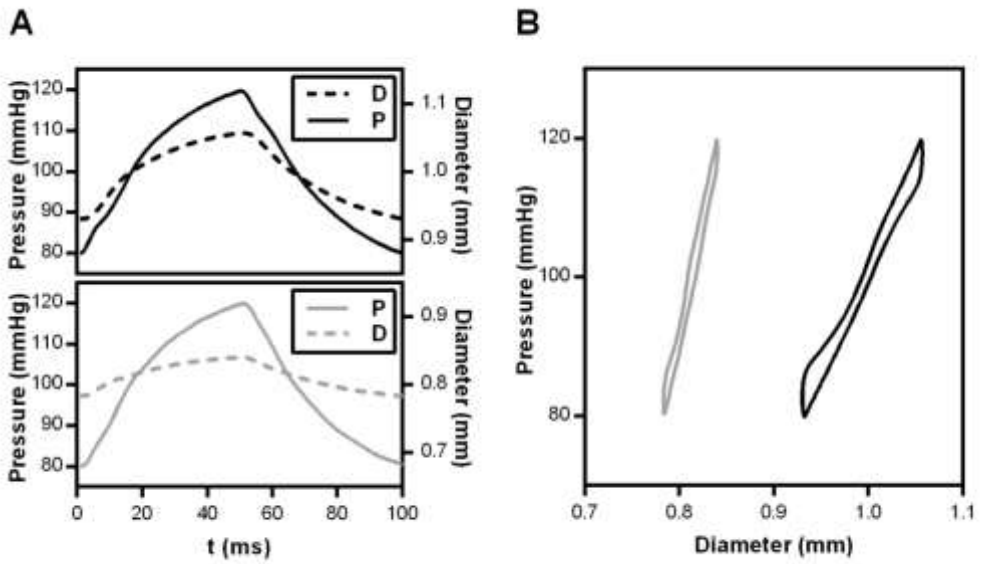

Figure 3. Processing of the data obtained from a compliant and stiff vessel segment. The graphs show examples of a WT aortic segment, either fully contracted using 1 µM PE and 300 µM L-NAME (stiff), or in Krebs-Ringer solution (compliant). Pressure (solid line) and diameter (dashed line) are plotted against time (A). As shown, segments were stretched between 80 and 120 mmHg at a stretch frequency of 10 Hz. When pressure and diameter are plotted against each other, a typical hysteresis loop was obtained (B). Compliant (black) and stiff (grey) vessel segments are shown to illustrate the differences in distension with similar pressure changes (A) and the difference in slope of the pressure-diameter loops (B).

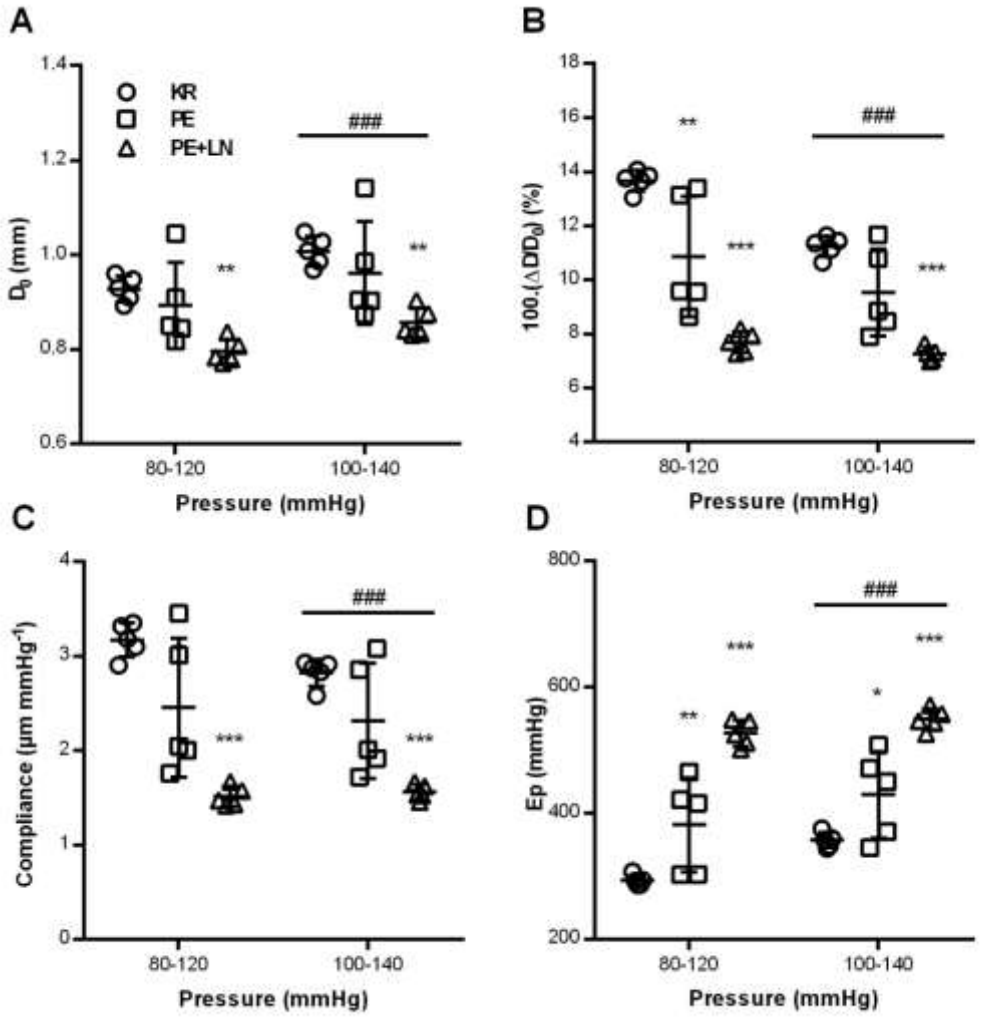

Figure 4. Isobaric vessel parameters under conditions with different VSMC tone and pressure. Diastolic diameter (D_0) (A), relative distension (B), compliance (C) and Peterson modulus (Ep) (D) were measured at physiological stretch frequency (10 Hz), either at normal pressure (80-120 mmHg) or at high pressure (100-140 mmHg). KR: Krebs-Ringer, PE: 1 µM phenylephrine, PE+LN: 1 µM phenylephrine + 300 µM L-NAME. *p<0.05, **p<0.01, ***p<0.001 (effect of VSMC tone, vs KR), ###p<0.001 (effect of pressure, vs NP), two-way ANOVA with Repeated Measures for pressure factor, Bonferroni post-hoc test (n=5).

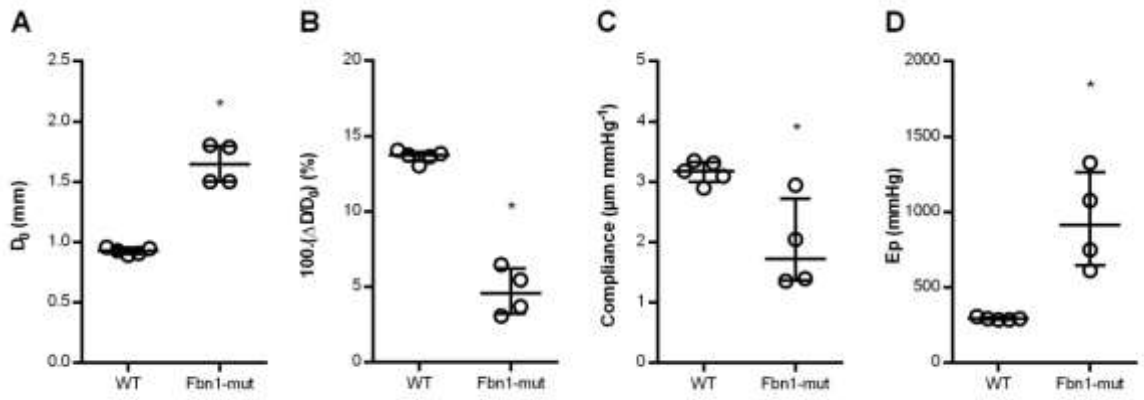

Figure 5. Comparison between WT mice (n=5) and mice with a heterozygous mutation of the Fbn1 gene (n=4). The aorta was dilated, as indicated by increased diastolic diameter (D_0) (A). Relative distension (B) and compliance (C) were significantly lower and Peterson modulus (Ep) was significantly increased (D). Measurements were done at physiological pressure range (80-120 mmHg) and stretch frequency (10 Hz). Line and error bars represent median and interquartile range, respectively. *p<0.05, Mann Whitney U test.

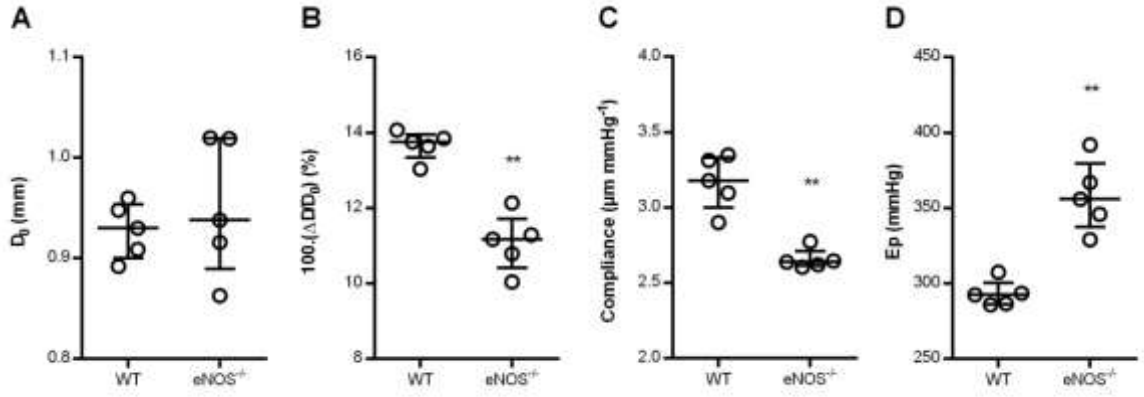

Figure 6. Geometrical and biomechanical parameters of eNOS$^{-/-}$ mice aortic segments. Increased aortic stiffness was confirmed in eNOS$^{-/-}$ mice (n=5). Although diastolic diameter (D_0) was similar to wild-type (WT) mice (n=5) (A), relative distension (B), compliance (C) and Peterson's modulus (Ep) (D) were significantly different. Measurements were done at a physiological pressure range (80-120 mmHg) and stretch frequency (10 Hz). Line and error bars represent median and interquartile range, respectively. **p<0.01, Mann Whitney U test.

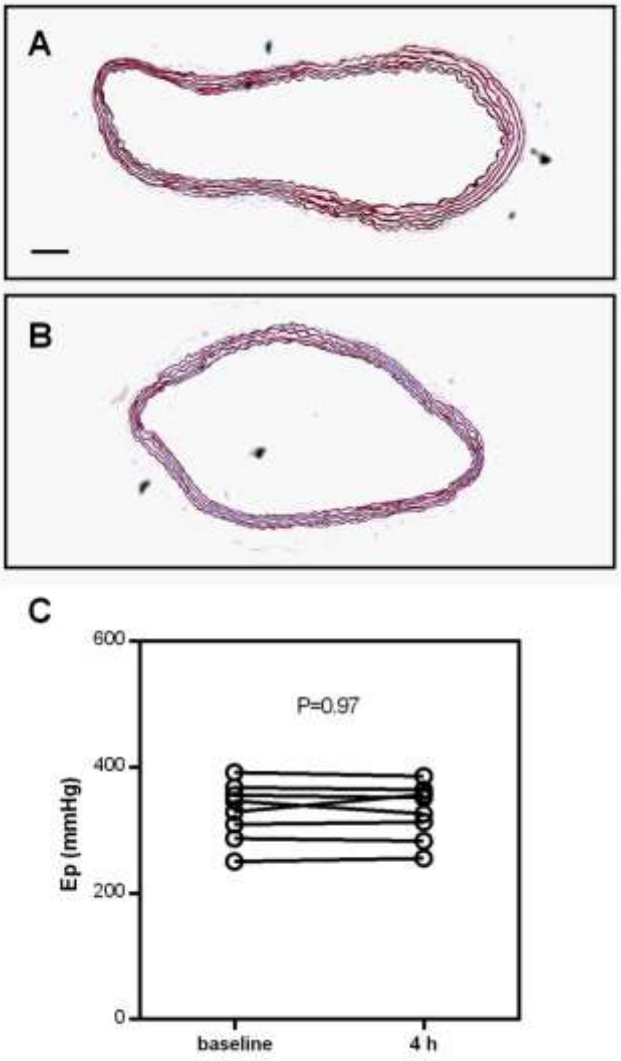

Figure 7. Effect of repetitive stretch on elastin fibre integrity and Ep. Orcein-stained section of aortic segments of WT mice after being mounted in the ROTSAC set-up at physiological pressure. The integrity of the elastin fibres after 4 hours of stretching at 10 Hz (A) was similar to when no stretch was applied (B). Ep at 80-120 mmHg was unchanged (P=0.97, paired t-test) (C) after 4 hours of stretching in a group of randomly selected mice with different baseline values of Ep (WT (n=3), $eNOS^{-/-}$ (n=5), P=0.97, paired t-test). Scale bar: 100 µm.